ChemComm

COMMUNICATION

View Article Online
View Journal | View Issue

Cite this: *Chem. Commun.*, 2021, 57, 191

Received 6th November 2020,
Accepted 24th November 2020

DOI: 10.1039/d0cc07333d

rsc.li/chemcomm

Structure–direction towards the new large pore zeolite NUD-3†

Fei-Jian Chen, ‡[a] Zihao Rei Gao, ‡[b] Jian Li, *[c] Luis Gómez-Hortigüela, [d] Cong Lin, [e] Le Xu, [e] Hong-Bin Du, *[f] Carlos Márquez-Álvarez, [d] Junliang Sun [e] and Miguel A. Camblor *[b]

The new zeolite NUD-3 possesses a three-dimensional system of large pore channels that is topologically identical to those of ITQ-21 and PKU-14. However, the three zeolites have distinctly different frameworks: a particular single 4-membered ring inside the denser portion of the zeolite is missing in PKU-14, disordered in ITQ-21 and fully ordered in NUD-3. We document these differences and use molecular simulations to unravel the mechanism by which a particular structure directing agent dication, 1,1′-(1,2-phenylenebis(methylene))bis(3-methylimidazolium), is able to orient this inner ring.

Structure directing agents (SDAs) typically play an important role in the synthesis of zeolites.[1,2] Over the last several decades there has been huge experimental effort in the design and trial of organic SDAs for the synthesis of zeolites.[3] The effort has been rewarded with a large increase in the number of zeolite topologies recognized as unique and viable by the International Zeolite Association (IZA) with a steady rate of over five new topologies accepted per year during the last 40 years.[4] However, it is still generally impossible to predict the target zeolite topology before the synthesis, even when the structural relationship among the various zeolite topologies and their "synthesis descriptors" is studied,[5] or when the SDA is selected by energy minimization calculations to target a specific topology,[6] although some notable cases of success have been reported.[7] Occasionally, a very small change in the SDA brings about a large change in the ability to produce one or another zeolite framework.[8] One could be tempted to consider structure–direction in pretty simple terms: zeolites that are intrinsically stable may just require a loose pore filling, easily achievable, for instance, by flexible SDAs that can adapt themselves to the zeolite pores ("the cation adapts to the pore", as in the so called "default zeolites"[9]), whereas less stable zeolites would require a more specific structure–direction where the pore matches to some extent the geometry of a particular cation ("the zeolite adapts to the cation"). However, the structure–direction by organic agents is far from well understood and it is likely rich in subtleties, although the notion that the size and shape of the organic cation may influence the size and shape of the zeolite pore in which it resides is still popular. We will challenge this notion by presenting the case of three zeolites with distinct structures but topologically identical pores that are synthesized through the use of different cations.

The new zeolite NUD-3 (Nanjing University Du's group zeolite number 3) possesses a hitherto unknown topology that is, however, closely related to those of another two previously reported materials, ITQ-21[10] and PKU-14.[11] In fact, the three zeolites possess a topologically identical three-dimensional (3D) system of large pores opened through 12-membered ring windows (12MR). The difference between the three materials doesn't lie in the pores but in the denser portion of the structure, where there may be missing tetrahedral atoms (PKU-14), a disordered array of atoms (ITQ-21) or a fully ordered structure (NUD-3). Since the pores of the three zeolites are topologically identical, it is intriguing that the ability to direct the synthesis towards any of the three materials depends on the host–guest interactions established between the cation and the pore. In this work, we characterize the new zeolite NUD-3 to clearly establish its unique nature and then use molecular simulations to study the mechanism of this special structure–direction effect.

[a] *Department of Chemistry, Bengbu Medical College, Bengbu 233030, China*
[b] *Instituto de Ciencia de Materiales de Madrid, Consejo Superior de Investigaciones Científicas (ICMM-CSIC) c/Sor Juana Inés de la Cruz 3, Madrid 28049, Spain. E-mail: macamblor@icmm.csic.es*
[c] *Berzelii Center EXSELENT on Porous Materials, Department of Materials and Environmental Chemistry, Stockholm University, Stockholm, 10691, Sweden. E-mail: jxpxlijian@pku.edu.cn*
[d] *Instituto de Catálisis y Petroleoquímica, Consejo Superior de Investigaciones Científicas (ICP-CSIC), c/Marie Curie 2, Madrid 28049, Spain*
[e] *College of Chemistry and Molecular Engineering, Peking University, 5 Yiheyuan Road, Beijing, 100871, China*
[f] *State Key Laboratory of Coordination Chemistry, School of Chemistry and Chemical Engineering, Nanjing University, Nanjing, 210023, China. E-mail: hbdu@nju.edu.cn*

† Electronic supplementary information (ESI) available: Experimental section, characterization methods, crystallographic details, computational details, and supplementary tables, figures and references. See DOI: 10.1039/d0cc07333d

‡ These authors contributed equally to this work.

NUD-3 has been discovered using 1,1′-(1,2-phenylenebis(methylene))bis(3-methylimidazolium) dications (**SDA1**, Fig. S1a, ESI†) and fluoride anions from a gel composition 0.5 SiO_2 : 0.5 GeO_2 : 0.25 $SDA(OH)_2$: 0.5 HF : 1.5 H_2O, at 150 °C for 15 days within a static autoclave. It is worth mentioning that one very similar **SDA2** (Fig. S1b, ESI†) was used by Boal *et.al.*, but only yielded a layered material plus zeolite Beta.[8c] Additionally, we have found out that, under the same synthesis conditions, **SDA3** (Fig. S1c, ESI†) and **SDA4** (Fig. S1d, ESI†), also containing phenyl and imidazolium moieties, are good templates to synthesize ITQ-21, but not NUD-3 (see the ESI,† Table S1).[12] An SDA similar to **SDA3** but lacking all methyl groups at position 2 of the imidazolium rings directed the synthesis towards ITQ-37 quite specifically.[13]

The structure of NUD-3 was solved by the state-of-the-art three-dimensional electron diffraction technique, namely continuous rotation electron diffraction (cRED).[14] A 4/*mmm* Laue symmetry with a tetragonal unit cell a = 14.56 Å and c = 13.11 Å can be easily obtained from the cRED dataset (Fig. S2, ESI†). The reflection conditions derived from the reconstructed 3D reciprocal lattice indicated as possible space groups *P*422 (89#), *P*4*mm* (99#), $P\bar{4}2m$ (111#), $P\bar{4}m2$ (115#) and *P*4/*mmm* (123#). The cRED data were used to solve the structure with space group *P*4/*mmm* and the structure, including the SDA location, was refined against synchrotron powder X-Ray diffraction data (Fig. S3, ESI†). All the crystallographic details are provided in the ESI† (Tables S2–S4, ESI†) and the structure was deposited in the CCDC (no. 2045881).

The framework of NUD-3 is very similar to those of ITQ-21 and PKU-14. Their structures could be described as 0D [$4^6 6^{12}$] units of 32 T atoms (*i.e.* units displaying six 4MR and twelve 6MR faces; T atoms: tetrahedral atoms) connected through double 4-membered rings (D4R) along the three dimensions, thus forming a 3D framework with intersecting 12MR channels along the three crystallographic axes (Fig. 1a and b). It should be noted that the only topological difference among NUD-3, ITQ-21 and PKU-14 is the presence, orientation or absence of four additional inner T atoms in that unit, which then may actually contain 32 or 36 T atoms. In ITQ-21, a single 4-membered ring unit (S4R) formed by those four inner atoms is disordered along the *a*-, *b*-, and *c*-axis, so each S4R has an occupancy of 1/3 and the unit contains 36 T atoms (Fig. 1d).[10] In PKU-14, the four inner atoms are absent and the unit is effectively a 32 T-atom cage filled with 8 terminal T–OH and 2 extra water molecules (Fig. 1e).[11] In contrast, in NUD-3, the four inner atoms form a S4R, which is ordered and oriented perpendicular to the *c*-axis (Fig. 1c), and the unit is a 36 T-atom unit. Since the structural difference between the three frameworks is restricted to an area inside a dense portion of the structure, the pore system and the microporous surface of the three zeolites are topologically equivalent, which makes intriguing that a simple host–guest filling interaction in the pores might cause a difference in the zeolite that crystallizes.

NUD-3 has a 3D system of intersecting and straight 12MR channels along the *a*-, *b*- and *c*-axis. Along the *a*- and *c*-axis (Fig. S4, ESI†), the pore sizes are 6.3 × 8.1 Å and 7.7 × 8.0 Å, respectively. The framework density (FD) of NUD-3 is 13.63 T/1000 Å^3, which is very close to that of ITQ-21 (13.55).[10b] N_2 and Ar adsorption data (Fig. S5–S7) are discussed in the ESI.†

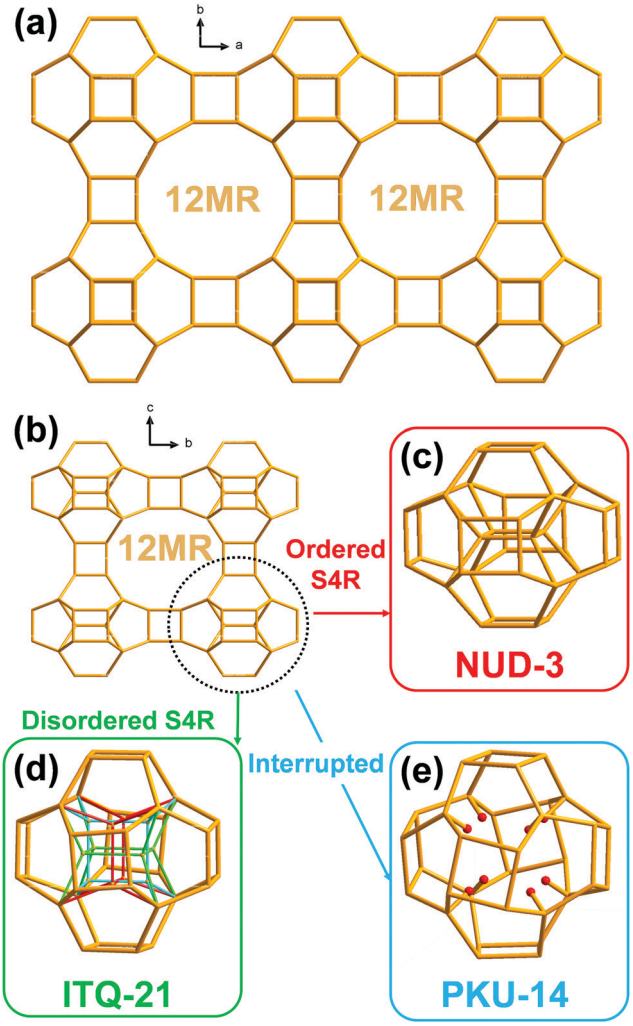

Fig. 1 Structural relationship among NUD-3, ITQ-21, and PKU-14: (a) 12MR channel in all three structures, viewed along the *c*-axis, (b) 12MR channel in NUD-3 with ordered S4R, viewed along the *a*-axis, where the 36 T unit is encircled, (c) the unit of 36 T atoms in NUD-3, showing the ordered S4R, (d) the unit of 36 T atoms in ITQ-21, with a S4R disordered along each direction and a 1/3 occupancy each (red, green and light blue), and (e) the unit of 32 T atoms in PKU-14, showing the absence of S4R and the presence of 8 terminal T–OH inside the resulting cage.

The differences between NUD-3, ITQ-21 and PKU-14 are clearly revealed in the PXRD patterns of the three structures and their symmetries (Fig. 2 and Table S5, ESI†). As-made and calcined ITQ-21 are cubic, $Fm\bar{3}c$, only showing three reflections, (200), (220) and (222), in the region up to 12° (Fig. 2a). As-made PKU-14 is monoclinic, *I*2/*m*, which splits the first and second peaks into several partially overlapped peaks (Fig. 2c). However, after heating PKU-14 at 180 °C for 2 hours, the removal of the water molecule inside the [$4^6 6^{12}$] cage results in a cubic symmetry with space group $Fm\bar{3}c$ (Fig. 2b),[11] the resulting pattern being much similar to that of ITQ-21 with the same three reflections in the low angle region. This high symmetry reflects the disorder inside the denser portion of both frameworks. By contrast, both as-made and calcined NUD-3 are tetragonal, space group *P*4/*mmm*, due to the ordered orientation of S4R, and thus the first two reflections (200)

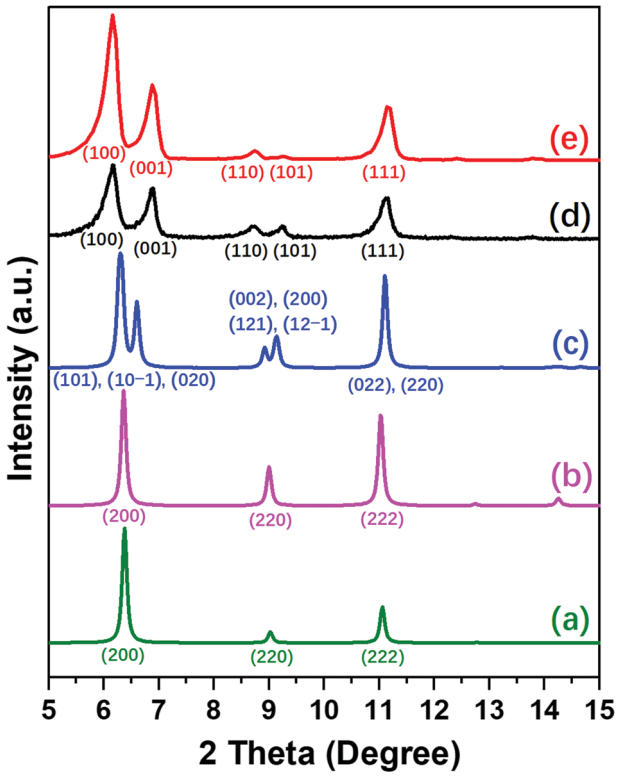

Fig. 2 PXRD patterns of simulated (a) as-made ITQ-21, (b) dehydrated PKU-14, (c) as-made PKU-14, and experimental (d) as-made NUD-3 and (e) calcined NUD-3. Each peak ranging from 2θ 5–15° is marked with its Miller index.

and (220) in the cubic system split into (100), (001) and (110), (101), respectively (Fig. 2d and e). Additionally, when we calcined the NUD-3 samples in air from room temperature to 600 °C, all the patterns kept the same tetragonal symmetry (Fig. S8, ESI†). In conclusion, the three structures can be characterized and distinguished by the differences in their PXRD patterns and crystallographic data.

The Fourier transform infrared (FT-IR) spectra can additionally prove the difference between NUD-3 and PKU-14. After heating at 180 °C for 2 hours, the FT-IR spectrum of NUD-3 (Fig. S9, ESI†) showed no band in the 3400–3600 cm^{-1} range while PKU-14 showed a band located at 3528 cm^{-1} ascribed to the stretching vibrations of the terminal hydroxyl groups.[11]

The incorporation of **SDA1** within the NUD-3 framework was studied by molecular simulations. We started from the location of the organic dication obtained from the Rietveld refinement; in this location, the organic dication sites in the *ac* (or *bc*) plane, with one imidazolium ring in the elliptical [100] (or [010]) channels, and the other imidazolium ring aligned along the *c*-axis (Fig. S10, ESI†). Three different long-range arrangements for packing the organic cations in such a position while avoiding short-contacts were found, which differ in the relative orientation of adjacent SDA1 cations (1, 2 and 3 in Fig. S11, ESI†). In the most stable case (3) (as calculated using Dreiding forcefield), the imidazolium rings along the *c* axis point in opposite directions, and no π–π stacking between imidazolium rings is developed (Fig. 3, top). From these systems with the NUD-3 framework

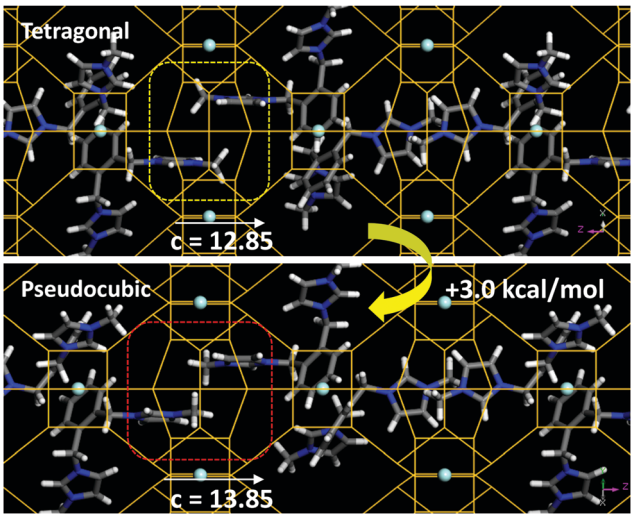

Fig. 3 Packing interactions between imidazolium rings along the [001] channels in the tetragonal (top) or pseudocubic (bottom) cell, showing the steric repulsion in the latter case.

under the Rietveld refined tetragonal unit cell, we built analogous systems but now with an isometric (pseudocubic) unit cell (with a = 13.8490 Å), and calculated the interaction energy (Table S6, ESI†). In all cases, the host/guest interaction energy developed in the pseudocubic framework is lower in magnitude, showing that **SDA1** fits better in the tetragonal framework. In order to confirm this, we built hypothetical NUD-3 frameworks while varying the c parameter from 12.35 to 14.85 Å, and calculated the stability of the resulting structure (Fig. S12, ESI†). Energy results showed a reduced stability when c increased, displaying an energy minimum at the real c value of 12.85 Å, clearly evidencing an optimal geometric relationship of **SDA1** and the NUD-3 tetragonal unit cell. Methyl groups in adjacent **SDA1** cations of the imidazolium rings aligned with [001] channels become too close when c increases (Fig. 3, bottom), provoking a steric repulsion and providing a potential explanation for the reduced stability of **SDA1** confined in the pseudocubic framework.

As mentioned previously, the reduced c parameter is a direct consequence of the ordered nature of the S4R, and hence of the better fit of the **SDA1** packing arrangement within a tetragonal unit cell. Propagation of this favored geometrical host/guest fit along the crystal might be explained because of the particular organic supramolecular arrangement, where the imidazolium rings aligned within the [001] channels develop a well-ordered orientation, with the imidazolium rings of adjacent cations siting parallel to each other to optimize the packing efficiency, spreading the preferred S4R orientation along the *c*-axis. In addition, adjacent **SDA1** cations in the *ab* plane orient perpendicular to each other to avoid overlapping (Fig. S11, ESI†), thus promoting also propagation of the preferred S4R orientation along the crystal in [100] and [010] directions. We note here that under none of the three potential configurations, π–π stacking interactions between the phenyl rings are established, which is consistent with a major occurrence of phenyl

monomers observed by fluorescence spectroscopy (band at 280 nm, Fig. S13, ESI†). Interestingly, this type of long-range organic arrangement achieved by **SDA1** is not possible for **SDA3** or **SDA4** because of their different molecular structure, which could explain the lack of a preferential long-range orientation of the zeolite building units, and hence the crystallization of a cubic framework with disordered S4R instead.

NUD-3 poses an additional intriguing question related to charge balance. In our **SDA1**-NUD-3 model, there are 2 dications per unit cell, which amounts to 4 positive charges. The organic content in the real system, impossible to model by simulation because of disorder, is even slightly larger. Three of the positive charges would be compensated by three F anions occupying the three D4Rs per unit cell found in the NUD-3 framework, consistent with a ^{19}F MAS NMR resonance at −8.2 ppm (Fig. S14, ESI†) that we assign to fluoride occluded in D4R units with Ge–Ge pairs but with no Ge adjacent to three Ge neighbours (type III resonance).[15] The rest of the positive charges could be balanced by T–O$^-$ but these are more frequently associated with T–OH that are absent in NUD-3,[16] according to the FT-IR spectra commented above. Thus, we propose that additional fluoride anions could be located in the main channels, associated with water clusters or the positively charged imidazolium rings, and could be responsible for an additional broad signal around −100 ppm in the ^{19}F MAS NMR spectrum. A broad signal around a similar chemical shift is present in the spectrum of PKU-12, where fluoride is believed to be present in 8MR pores (in addition to D4R).[17]

In conclusion, NUD-3 possesses a new topology with a 3D system of large pores. The structure is fully ordered and fully condensed and is closely related to the disordered zeolite ITQ-21 and the interrupted zeolite PKU-14. Its structure has been solved by continuous rotation electron diffraction and refined using synchrotron diffraction data. We propose that the ability of the SDA to direct the crystallization to a fully ordered, fully condensed tetragonal framework relies on better packing of the organic structure directing agent in the tetragonal cell. This can explain the specific structure–direction of **SDA1** towards NUD-3 despite the topological equality of the pore system of the three zeolites.

The authors are grateful for financial support from the Spanish Ministry of Science Innovation and Universities (MAT2015-71117-R, PID2019-105479RB-I00 and PID2019-107968RB-I00 projects, AEI, Spain and FEDER, EU), the National Natural Science Foundation of China (No. 22071099, 21673115, 21527803, 21871009, and 21601004), top talent cultivation program of Anhui Educational Committee (gxgwfx2018051), and the Swedish Research Council (VR) and the Knut and Alice Wallenberg Foundation (KAW). Synchrotron experiments were performed at beamline BL04 (MSPD) at ALBA Synchrotron with the collaboration of ALBA staff, and special thanks are given to A. Manjón for support in collecting the data and for helpful comments and suggestions. Z. R. G. specially thanks Yingxia Wang of Peking University for her kind suggestions and help with this paper. Centro Técnico Informático-CSIC is acknowledged for running the calculations, and BIOVIA for providing the computational software. We acknowledge support of the publication fee by the CSIC Open Access Publication Support Initiative through its Unit of Information Resources for Research (URICI).

Conflicts of interest

There are no conflicts to declare.

Notes and references

1 R. F. Lobo, S. I. Zones and M. E. Davis, *J. Inclusion Phenom. Macrocyclic Chem.*, 1995, **21**, 47–78.
2 L. Gómez-Hortigüela and M. A. Camblor, Insights Into The Chemistry Of Organic Structure-Directing Agents In The Synthesis Of Zeolitic in *Materials*, ed. L. Gómez-Hortigüela, Springer, 2018, 175, pp. 1–42.
3 *Insights into the Chemistry of Organic Structure-Directing Agents in the Synthesis of Zeolitic Materials*, ed. L. Gómez-Hortigüela, Springer, 2018, p. 175.
4 C. Baerlocher and L. B. McCusker, Database of Zeolite Structures, 2020, http://www.iza-structure.org/databases.
5 K. Muraoka, Y. Sada, D. Miyazaki, W. Chaikittisilp and T. Okubo, *Nat. Commun.*, 2019, **10**, 4459.
6 C.-R. Boruntea, G. Sastre, L. F. Lundegaard, A. Corma and P. N. R. Vennestrøm, *Chem. Mater.*, 2019, **31**(22), 9268–9276.
7 (*a*) J. E. Schmidt, M. W. Deem and M. E. Davis, *Angew. Chem.*, 2014, **126**, 8512–8514 (*Angew. Chem., Int. Ed.*, 2014, **53**, 8372–8374); (*b*) S. K. Brand, J. E. Schmidt, M. W. Deem, F. Daeyaert, Y. Ma, O. Terasaki, M. Orazov and M. E. Davis, *Proc. Natl. Acad. Sci. U. S. A.*, 2017, **114**(20), 5101–5106.
8 (*a*) A. Rojas, L. Gomez-Hortiguela and M. A. Camblor, *Dalton Trans.*, 2013, **42**, 2562–2571; (*b*) B. W. Boal, M. W. Deem, D. Xie, J. H. Kang, M. E. Davis and S. I. Zones, *Chem. Mater.*, 2016, **28**(7), 2158–2164; (*c*) J. E. Schmidt, C.-Y. Chen, S. K. Brand, S. I. Zones and M. E. Davis, *Chem. – Eur. J.*, 2016, **22**, 4022–4029; (*d*) P. Lu, L. Villaescusa and M. A. Camblor, *Chem. Rec.*, 2018, **18**, 713–723; (*e*) L. Villaescusa, J. Li, Z. Gao, J. Sun and M. A. Camblor, *Angew. Chem.*, 2020, **132**, 11379–11382 (*Angew. Chem., Int. Ed.*, 2020, **59**, 11283–11286); (*f*) Z. R. Gao, J. Li, C. Lin, A. Mayoral, J. Sun and M. A. Camblor, *Angew. Chem.*, DOI: 10.1002/anie.202011801.
9 A. Moini, K. D. Schmitt, E. W. Valyocsik and R. F. Polomski, *Zeolites*, 1994, **14**(7), 504–511.
10 (*a*) A. Corma, M. J. Diaz-Cabanas, J. Martinez-Triguero, F. Rey and J. Rius, *Nature*, 2002, **418**, 514–517; (*b*) T. Blasco, A. Corma, M. J. Diaz-Cabanas, F. Rey, J. Rius, G. Sastre and J. A. Vidal-Moya, *J. Am. Chem. Soc.*, 2004, **126**, 13414–13423.
11 J. Liang, J. Su, Y. Wang, Y. Chen, X. Zou, F. Liao, J. Lin and J. Sun, *Chem. – Eur. J.*, 2014, **20**, 16097–16101.
12 F.-J. Chen, *Rational Design and Application of Structure-Directing Agents for Zeolite Synthesis*, PhD thesis, Nanjing University, Nanjing, 2014.
13 F.-J. Chen, Z.-H. Gao, L.-L. Liang, J. Zhang and H.-B. Du, *CrystEngComm*, 2016, **18**, 2735–2741.
14 (*a*) J. Li and J. Sun, *Acc. Chem. Res.*, 2017, **50**(11), 2737–2745; (*b*) Z. Huang, E. S. Grape, J. Li, K. Inge and X. Zou, *Coord. Chem. Rev.*, 2021, **427**, 213583.
15 R. T. Rigo, S. R. G. Balestra, S. Hamad, R. Bueno-Perez, A. R. Ruiz-Salvador, S. Calero and M. A. Camblor, *J. Mater. Chem. A*, 2018, **6**, 15110–15122.
16 H. Koller, R. F. Lobo, S. L. Burkett and M. E. Davis, *J. Phys. Chem.*, 1995, **99**, 12588–12596.
17 J. Su, Y. Wang, J. Lin, J. Liang, J. Sun and X. Zou, *Dalton Trans.*, 2013, **42**, 1360–1363.

